Mathematical Biosciences and Engineering

http://www.aimspress.com/journal/mbe

MBE, 20(2): 3838–3853.
DOI: 10.3934/mbe.2023180
Received: 05 October 2022
Revised: 12 November 2022
Accepted: 02 December 2022
Published: 12 December 2022

Research article

Breast cancer chemical structures and their partition resolvability

Qingqun Huang[1], Adnan Khalil[2], Didar Abdulkhaleq Ali[3], Ali Ahmad[4], Ricai Luo[1] and Muhammad Azeem[5,*]

[1] School of Mathematics and Physics, Hechi University, Yizhou, Guangxi 456300, China
[2] Department Computer Sciences, Al-Razi Institute Saeed Park, Lahore Pakistan
[3] Department of Mathematics, Faculty of Science, University of Zakho, Zakho, Iraq
[4] College of Computer Science & Information Technology, Jazan University, Jazan, Saudi Arabia
[5] Department of Mathematics, Riphah International University Lahore, Pakistan

* **Correspondence:** Email: azeemali7009@gmail.com; Tel: +923005067913.

Abstract: Cancer is a disease that causes abnormal cell formation and spreads throughout the body, causing harm to other organs. Breast cancer is the most common kind among many of cancers worldwide. Breast cancer affects women due to hormonal changes or genetic mutations in DNA. Breast cancer is one of the primary causes of cancer worldwide and the second biggest cause of cancer-related deaths in women. Metastasis development is primarily linked to mortality. Therefore, it is crucial for public health that the mechanisms involved in metastasis formation are identified. Pollution and the chemical environment are among the risk factors that are being indicated as impacting the signaling pathways involved in the construction and growth of metastatic tumor cells. Due to the high risk of mortality of breast cancer, breast cancer is potentially fatal, more research is required to tackle the deadliest disease. We considered different drug structures as chemical graphs in this research and computed the partition dimension. This can help to understand the chemical structure of various cancer drugs and develop formulation more efficiently.

Keywords: resolvability parameters; breast cancer structures; resolving set; locating set; locating number; partition resolving set

1. Introduction

Trillions of cells make up the human body. Cell division occurs naturally in all living things. Cancer develops when uncontrollable cell division occurs and spreads to neighboring tissues, forming tumors. Cancer can occur in any region of the body. Patient recovery rates have significantly improved in recent years. Cancer develops as a result of hormonal or genetic alterations in the DNA. Cancer affects

people of all ages, from babies to the elderly, although it most commonly affects adults. A biopsy is essential to confirm the diagnosis if another growth, lump, or tumor appears in the body. Tumors may be cancerous or benign. Benign non-cancerous tumors do not spread to neighboring tissues. Certain benign tumors, on the other hand, can be lethal if they form in the brain.

The chance of acquiring cancer can be reduced by various variables, including keeping a healthy lifestyle, avoiding cancer-causing foods, and receiving cancer-prevention vaccinations. Tobacco use, carcinogen exposure, and cooking with Teflon-coated utensils are all carcinogens with the potential to produce the worst illness [1–3].

Cancer affects all humans, regardless of gender. Women are disproportionately impacted by breast and cervical cancer. According to 2020, million women worldwide were affected by breast cancer, with 685,000 losing their struggle against the worst illness. It is most commonly seen in the lining of milk ducts and the lobules that provide milk to these ducts. There are more than 18 types of breast cancer. Mammograms are used to detect breast cancer at an early stage. Clinical trials, immunological therapy, hormone therapy, targeted therapy, surgery, chemotherapy, and radiation therapy are all part of the treatment [4, 5].

Assume $G(V(G), E(G))$ is an undirected graph of a chemical structure (network), with $V(G)$ representing the set of primary nodes (vertex set) and $E(G)$ representing the set of branches (edge set). The distance between two primary nodes $v_1, v_2 \in V(G)$, abbreviated as $d(v_1, v_2)$, is the least number of edges between the v_1, v_2 route. Assume $R \subset V(G)$ is the subset of principal nodes defined by $R = \{v_1, v_2, \ldots, v_s\}$, and consider a principal node $v \in V(G)$. A primary node's identification or position $r(v|R)$ with regard to R is really a distance $(d(v, v_1), d(v, v_2), \ldots, d(v, v_s))$. If each primary node in $V(G)$ has a unique identity according to the ordered subset R, then this subset is termed a network resolving set. The metric of dimension is the minimal number of elements in the subset R, which is indicated by the word dim (G). Metric dimension is used in various applications, including combinatorial optimization, robot roving [6], complicated games, image processing, pharmaceutical chemistry, polymer production [7], and the electric field. These applications may all be found in [8–16].

The Authors examined windmill graphs in terms of metric generalization in their research work [17,18]. The authors explored the extended version of the measured dimension graph and characterized this parameter as a function of two variables. Researchers derived metrics and upper limits on various generalized families of graphs in [19]. Polycyclic hydrocarbons are discussed in depth in this [20], along with the notion of metric and its extensions. In [21], symmetric graphs are created using the rooted product, and metrics and their extensions are investigated. Researchers present the concept of the hollow coronoid on the metric dimension and its generalization [22]. The authors investigated and measured the resolvability of quartz structure and precisely calculated metric parameters for quartz structure without considering the pendant nodes beyond the circle.

The research of [23] provides information on rough graphs on the themes of metric dimensions and their generalized parameters. The authors of [24] studied hereditary bipartite networks and how to compute the metric basis of this extended class of complex networks. The concept of pseudo-valuation on KU-algebras was examined in the research work given in [25], as well as the link between pseudo-valuations and KU-algebras and their generalizations. More current publications on chemical networks [26–30], and the metric parameters of various chemical structures and networks may be found in [31–36]. In [37, 38], authors discussed some modeling and algorithms for that modeling regarding some disease and their cures.

Definition 1.1. *Let $R_p \subseteq V(G)$ is the s-elements proper set and $r(v|R_p) = d(v|R_{p_1}), d(v|R_{p_2}), \ldots, d(v|R_{p_s})$, is the s-tuple distance identification of a principal node v in association with R_p. If the entire set of principal nodes have unique identifications, then R_p is named as the partition resolving set of the principal node of a network G. The least possible count of the subsets in that set of $V(G)$ is labeled as the partition dimension pd of G.*

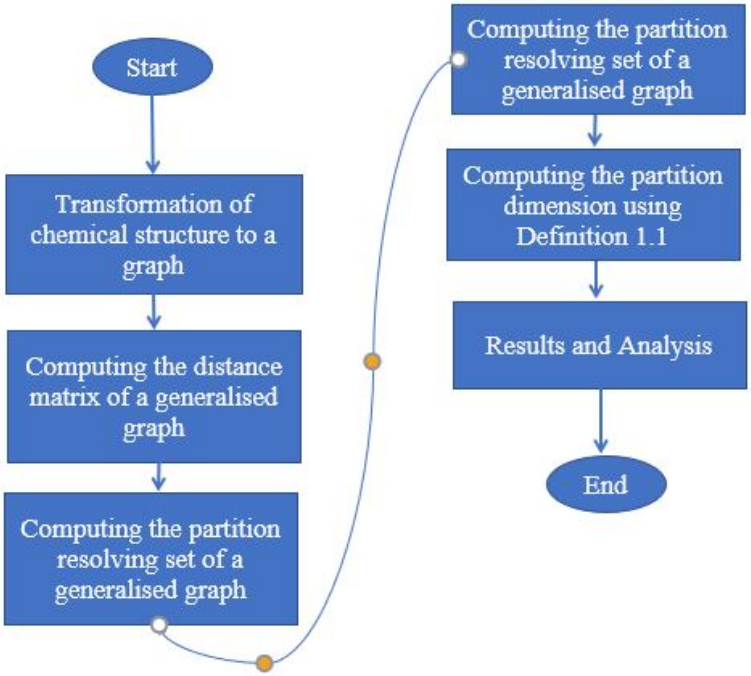

Figure 1. Flowchart for comouting the partition dimension of a chemical structure.

Further, the methodology is presented in Figure 1. Partition dimension is another type of dimension like metric dimension on the basics of vertices. Computing the metric dimension of different chemical structures is an NP-hard problem and adding the partition dimension is too. Because partition dimension has a more complicated structure than metric dimension, fewer precise partitions are accessible, and boundaries are frequently offered. Bounds for the partition of the generalized class of convex polytopes were reported in [39,40]. Presents a chemical fullerene graph, [41] details constraints on another chemical structure, [42] presents several nanotubes and sheets in the form of partition sets, and [43] provides the two-dimensional lattice structure.

Resolvability concepts are used in various applications, including combinatorial optimization, robot roving, complicated games, image processing, pharmaceutical chemistry, polymer production, and the electric field. These applications may all be found in [6, 7, 14–16].

2. Main results

We will include our findings of partition locating sets of various cancer drugs structures, such as Daunorubicin, Degualin, Minocyline, Podophylb toxin, Pterocevin, and Raloxifene.

Podophylb toxin structure's order and size are $\left|V\left(G\text{Podophylb toxin}\right)\right| = 30$, $\left|E\left(G\text{Podophylb toxin}\right)\right| = 33$, respectively. The node and bond set of the Podophylb toxin drug structure is shown below. Furthermore, Figure 3 depicts the molecular graph of Podophylb toxinl and labeling employed in our findings.

$$V\left(G_{\text{Podophylb toxin}}\right) = \{v_i : i = 1, 2, \ldots, 30\},$$
$$E\left(G_{\text{Podophylb toxin}}\right) = \{v_i v_{i+1} : i = 1, 2, \ldots, 15, 19, 20, \ldots, 23\} \cup \{v_4 v_{18},\ v_1 v_{16},$$
$$v_{19} v_{24},\ v_{21} v_{30},\ v_{29} v_{30},\ v_{22} v_{28},\ v_{27} v_{28},\ v_{23} v_{26},\ v_{25} v_{26},\ v_3 v_{15},\ v_5 v_{13}, v_7 v_{11}\}.$$

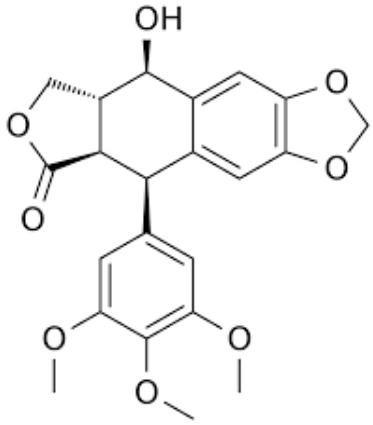

Figure 2. Chemical structure of Podophylb toxin drug.

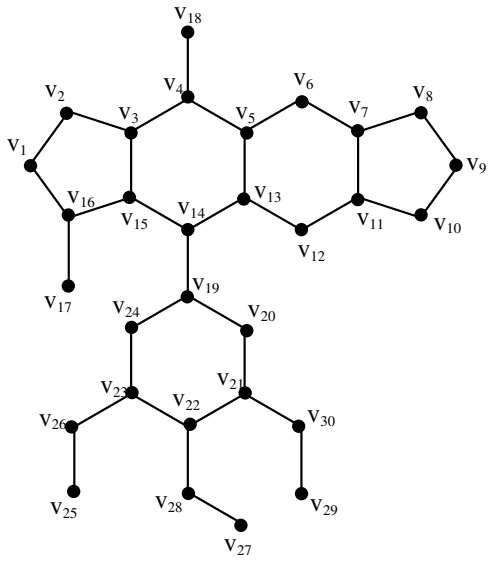

Figure 3. Graph of Podophylb toxin drug structure shown in the Figure 2.

Theorem 2.1. *Let G be a graph of Podophylb toxin drug structure. Then the partition dimension of G is* 3.

Proof. The graph's partition dimension of Podophylb toxin drug structure is 2. To demonstrate this point, we picked a partition locating set of cardinality 3 and stated as $R(G) = \{R_1, R_2, R_3\}$, where $R_1 = \{v_1\}$, $R_2 = \{v_{25}\}$ and $R_3 = V(G)\backslash\{v_1, v_{25}\}$. To demonstrate this statement true, we have included representations of each node of the Podophylb toxin drug structure except v_1 and v_{25} in Table 1.

Table 1. Representations of the nodes w.r.t. R.

$r(v_i\|R)$	R_1	R_2	R_3	Range of i
v_i	$i-1$	8	0	$i = 1, 4$
v_i	$i-1$	$11-i$	0	$i = 2$
v_i	$i-1$	$10-i$	0	$i = 3$
v_i	$i-1$	$i+2$	0	$i = 5, ..., 8$
v_i	$i-1$	$19-i$	0	$i = 9$
v_i	$17-i$	$19-i$	0	$i = 10, ..., 14$
v_i	$17-i$	$i-9$	0	$i = 15, 16$
v_i	$19-i$	$i-9$	0	$i = 17$
v_i	$i-15$	$i-15$	0	$i = 19, 20$
v_i	$i-15$	$25-i$	0	$i = 21, 22$
v_i	$29-i$	$i-21$	0	$i = 23, 24$
v_i	$33-i$	$27-i$	0	$i = 26$
v_i	$35-i$	$32-i$	0	$i = 27$
v_i	$36-i$	$32-i$	0	$i = 28$
v_i	$37-i$	$35-i$	0	$i = 29, 30$

Each node of graph of the Podophylb toxin medication structure's given positions is unique and meets the specifications of the partition locating set. This demonstrated that the partition locating number is correct.

Hence, proved that $pd\left(G_{\text{Podophylb toxin}}\right) \leq 3$. To verify this statement, we must demonstrate that $pd\left(G_{\text{Podophylb toxin}}\right) \geq 3$, and then by contradiction, we will have $pd\left(G_{\text{Podophylb toxin}}\right) = 2$.This is not correct because this assertion is only applicable to path graphs.

Hence, proved that $pd\left(G_{\text{Podophylb toxin}}\right) = 3$.

Pterocellin structure's order and size are $|V(G_{\text{Pterocellin}})| = 24$, $|E(G_{\text{Pterocellin}})| = 27$, respectively. The node and bond set of the Pterocellin drug structure are shown below. Furthermore, Figure 5 depicts the molecular graph of Pterocellin and labeling employed in our findings.

$$\begin{aligned} V(G_{\text{Pterocellin}}) =& \{v_i : i = 1, 2, \ldots, 24\}, \\ E(G_{\text{Pterocellin}}) =& \{v_i v_{i+1} : i = 1, 2, \ldots, 14, 18, 19 \ldots, 23\} \cup \{v_1 v_{13},\ v_1 v_{16}, \\ & v_3 v_{11},\ v_5 v_{10},\ v_9 v_{18},\ v_{19} v_{24},,\ v_4 v_{17}\}. \end{aligned}$$

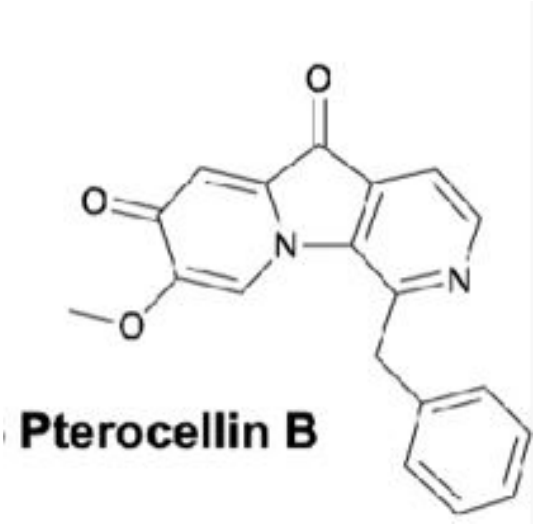

Figure 4. Chemical structure of Pterocellin toxin drug.

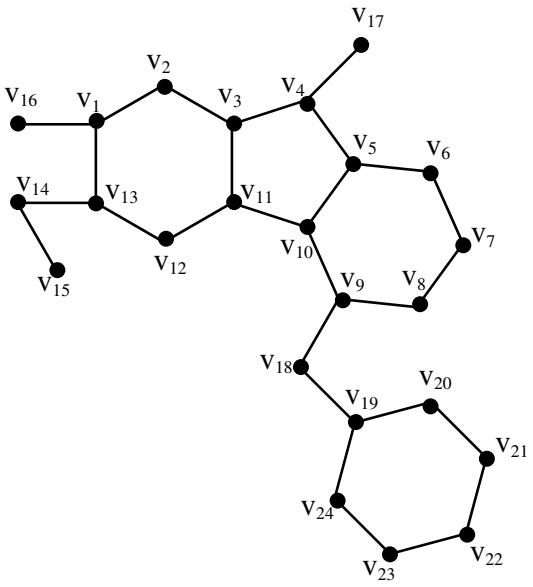

Figure 5. Graph of Pterocellin toxin drug structure shown in the Figure 4.

Theorem 2.2. *Let G be a graph of Pterocellin drug structure. Then the partition locating number of G is* 3.

Proof. The graph's partition dimension of Pterocellin drug structure is 3. To demonstrate this point, we picked a partition set of cardinality 3 and stated as $R(G) = \{R_1, R_2, R_3\}$, where $R_1 = \{v_2\}$, $R_2 = \{v_{20}\}$ and $R_3 = V(G)\backslash\{v_2, v_{20}\}$. To demonstrate this statement true, we have included representations of each node of the Pterocellin drug structure except v_2 and v_{20} in Table 2.

Table 2. Representations of the vertices with respect to R.

$r(v_i\|R)$	R_1	R_2	R_3	Range of i
v_i	i	$i+5$	0	$i=1$
v_i	$i-2$	$i+5$	0	$i=2,3$
v_i	$i-2$	$10-i$	0	$i=4,5$
v_i	$i-2$	$12-i$	0	$i=6,7$
v_i	$13-i$	$12-i$	0	$i=8$
v_i	$13-i$	$i-6$	0	$i=9,10,11$
v_i	$i-11$	$i-6$	0	$i=12,...,15$
v_i	$i-14$	$25-i$	0	$i=16$
v_i	$i-14$	$24-i$	0	$i=17$
v_i	$i-13$	$\|20-i\|$	0	$i=18,...,22$
v_i	$31-i$	$26-i$	0	$i=23,24$

Each node of graph of the Pterocellin medication structure's given positions is unique and meets the specifications of the partition locating set. This demonstrated that the partition locating number is correct.

Hence, proved that $pd(G_{\text{Pterocellin}}) \leq 3$. To verify this statement, we must demonstrate that $pd(G_{\text{Pterocellin}}) \geq 2$, and then by contradiction, we will have $pd(G_{\text{Pterocellin}}) = 2$. This is not correct because this assertion is only applicable to path graphs.

Hence, proved that $pd(G_{\text{Pterocellin}}) = 3$.

Daunorubicin structure's order and size are $|V(G_{\text{Daunorubicin}})| = 38$, $|E(G_{\text{Daunorubicin}})| = 42$, respectively. The node and bond set of the Daunorubicin drug structure are shown below. Furthermore, Figure 7 depicts the molecular graph of Daunorubicin and labeling employed in our findings.

$$
\begin{aligned}
V(G_{\text{Daunorubicin}}) =& \{v_i : i = 1,2,\ldots,38\},\\
E(G_{\text{Daunorubicin}}) =& \{v_iv_{i+1} : i = 1,2,\ldots,17,29,30\ldots,34\} \cup \{v_1v_{18},\ v_3v_{16},\\
& v_5v_{14},\ v_7v_{12},\ v_{13}v_{28},\ v_{15}v_{27},\ v_{17}v_{26},\ v_{25}v_{26},\ v_{11}v_{29},\ v_{32}v_{36},\\
& v_{33}v_{37},\ v_{34}v_{38},\ v_{30}v_{35},\ v_9v_{23},\ v_{22}v_{23},\ v_{21}v_{23},\ v_4v_{19},\ v_6v_{20},\ v_9v_{24}\}.
\end{aligned}
$$

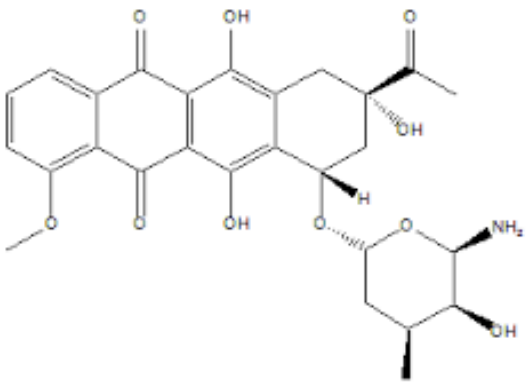

Figure 6. Chemical structure of daunorubicin drug.

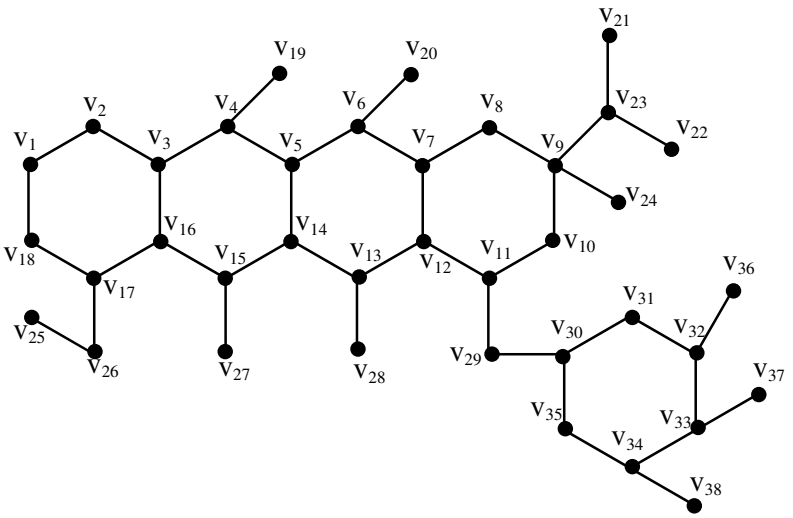

Figure 7. Graph of daunorubicin drug structure shown in the Figure 6.

Theorem 2.3. *Let G be a graph of Daunorubicin drug structure. Then the partition locating number of G is less than equal to* 4.

Proof. The graph's partition dimension or locating number of Daunorubicin drug structure is 4. To demonstrate this point, we picked a partition set of cardinality 4 and stated as $R(G) = \{R_1, R_2, R_3, R_4\}$, where $R_1 = \{v_1\}$, $R_2 = \{v_{21}\}$, $R_3 = \{v_{36}\}$ and $R_4 = V(G)\backslash\{v_1, v_{21}, v_{36}\}$.To demonstrate this statement true, we have included representations of each node of the Daunorubicin drug structure except v_1, v_{21} and , v_{36} in Table 3.

Table 3. Representations of the nodes with respect to R.

$r(v_i\|\chi)$	R_1	R_2	R_3	R_4	Range of i
v_i	$i-1$	$i-2$	$16-i$	0	$i = 2, .., 10$
v_i	$19-i$	$20-i$	$i-6$	0	$i = 11, ..., 18$
v_i	$23-i$	$22-i$	$32-i$	0	$i = 19$
v_i	$26-i$	$25-i$	$31-i$	0	$i = 20$
v_i	$31-i$	$31-i$	$30-i$	0	$i = 21$
v_i	$32-i$	$32-i$	$31-i$	0	$i = 22$
v_i	$29-i$	$30-i$	$38-i$	0	$i = 25, 26$
v_i	$32-i$	$33-i$	$37-i$	0	$i = 27$
v_i	$35-i$	$36-i$	$36-i$	0	$i = 28$
v_i	$i-20$	$i-19$	$33-i$	0	$i = 29, ..., 32$
v_i	$i-22$	$47-i$	$i-31$	0	$i = 33, ..., 35$
v_i	$51-i$	$52-i$	$41-i$	0	$i = 37$
v_i	$51-i$	$52-i$	$43-i$	0	$i = 38$

Each node of graph of the Daunorubicin medication structure's given positions is unique and meets

the specifications of the partition locating set. This demonstrated that the partition locating number was correct.

Hence, proved that $pd\left(G_{\text{Daunorubicin}}\right) \leq 4$.

Deguolin structure's order and size are $\left|V\left(G_{\text{Deguolin}}\right)\right| = 38$, $\left|E\left(G_{\text{Deguolin}}\right)\right| = 35$, respectively. The node and bond set of the Deguolin drug structure are shown below. Furthermore, Figure 8 depicts the molecular graph of Deguolin and labeling employed in our findings.

$$\begin{aligned} V\left(G_{\text{Deguolin}}\right) =& \{v_i : \ i = 1, 2, \ldots, 38\}, \\ E\left(G_{\text{Deguolin}}\right) =& \{v_i v_{i+1} : \ i = 1, 2, \ldots, 21\} \cup \{v_1 v_{22}, \ v_3 v_{20}, \\ & v_6 v_{19}, \ v_8 v_{17}, \ v_{14} v_9, \ v_{12} v_{28}, \ v_{12} v_{29}, \ v_{18} v_{30}, \\ & v_{19} v_{31}, \ v_{22} v_{26}, \ v_{25} v_{26}, \ v_1 v_{24}, \ v_{23} v_{24}, \ v_6 v_{27}\}. \end{aligned}$$

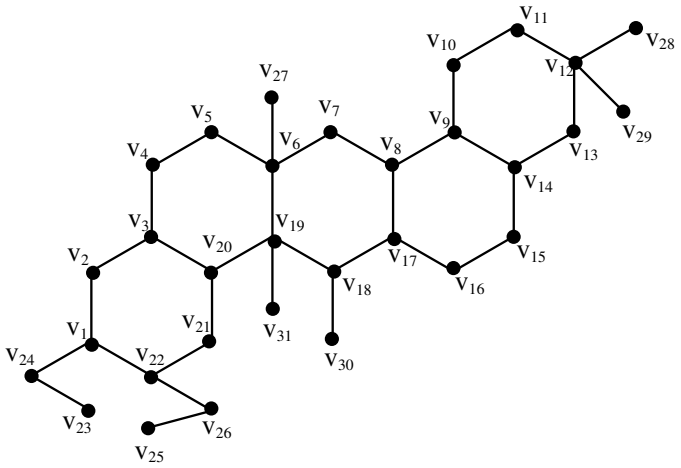

Figure 8. Deguolin drug structure.

Theorem 2.4. *Let G be a graph of Deguolin drug structure. Then the partition locating number of G is less than equal to* 4.

Proof. The graph's partition dimension or locating number of Deguolin drug structure is 4. To demonstrate this point, we picked a partition locating set of cardinality 4 and stated as

$R(G) = \{R_1, R_2, R_3, R_4\}$, where $R_1 = \{v_2\}$, $R_2 = \{v_{15}\}$, $R_3 = \{v_{28}\}$ and $R_4 = V(G)\backslash\{v_2, v_{15}, v_{28}\}$.To demonstrate this statement true, we have included representations of each node of the Deguolin drug structure except v_2, v_{15} and v_{28} in Table 4.

Table 4. Representations of the vertices with respect to R.

$r(v_i\|R)$	R_1	R_2	R_3	R_4	Range of i
v_i	$i-2$	$11-i$	$13-i$	0	$i=4,..,8$
v_i	$i-2$	$i-7$	$13-i$	0	$i=9,10$
v_i	$i-2$	$15-i$	$13-i$	0	$i=11$
v_i	$22-i$	$15-i$	$13-i$	0	$i=12$
v_i	$22-i$	$i-15$	$i-11$	0	$i=16,...,20$
v_i	$24-i$	$i-15$	$i-11$	0	$i=21,22$
v_i	$26-i$	$33-i$	$36-i$	0	$i=23,24$
v_i	$29-i$	$34-i$	$38-i$	0	$i=25,26$
v_i	$32-i$	$33-i$	$35-i$	0	$i=27$
v_i	$39-i$	$28-i$	$31-i$	0	$i=29$
v_i	$35-i$	$34-i$	$38-i$	0	$i=30$

Each node of graph of the Deguolin medication structure's given positions is unique and meets the specifications of the partition locating set. This demonstrated that the partition locating number was correct.

Hence, proved that $pd\left(G_{\text{Deguolin}}\right) \leq 4$.

The node and bond set of the Minocyline drug structure are shown below. This Minocyline structure's order and size are $\left|V\left(G_{\text{Minocycline}}\right)\right| = 35$, $\left|E\left(G_{\text{Minocycline}}\right)\right| = 38$, respectively. Furthermore, Figure 10 depicts the molecular graph of Minocyline and labeling employed in our findings.

$$
\begin{aligned}
V\left(G_{\text{Minocycline}}\right) =& \{v_i : \ i = 1, 2, \ldots, 35\},\\
E\left(G_{\text{Minocycline}}\right) =& \{v_i v_{i+1} : \ i = 1, 2, \ldots, 18\} \cup \{v_1v_{18},\ v_3v_{16}, v_5v_{14},\ v_7v_{12},\\
& v_2v_{23},\ v_3v_{24},\ v_4v_{25},\ v_6v_{26},\ v_8v_{27},\ v_1v_{21},\ v_{21}v_{22},\ v_{20}v_{21},\ v_{11}v_{29},\\
& v_{28}v_{29},\ v_{29}v_{30},\ v_{14}v_{31},\ v_{16}v_{32},\ v_{17}v_{34},\ v_{33}v_{34},\ v_{34}v_{35}\}.
\end{aligned}
$$

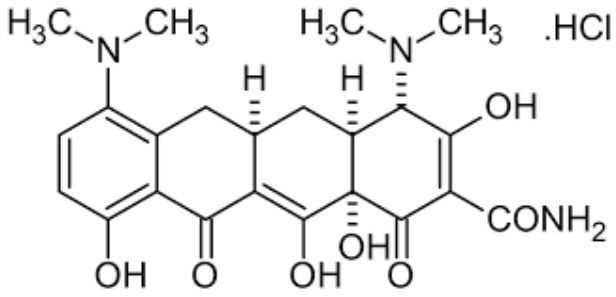

Figure 9. Chemical structure of Minocyline drug.

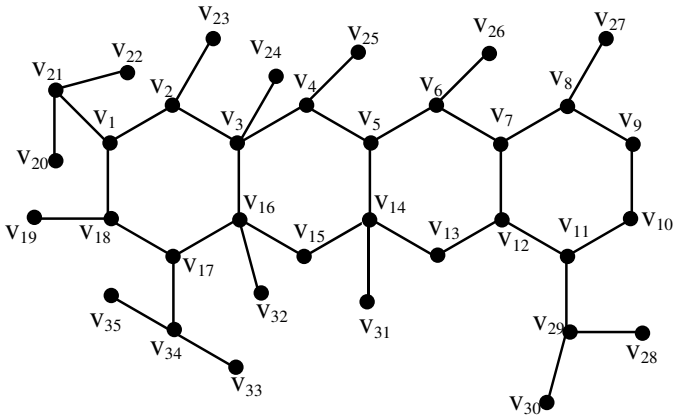

Figure 10. Graph Minocyline drug structure shown in the Figure 9.

Theorem 2.5. *Let G be a graph of Minocyline drug structure. Then the partition locating number of G is less than equal to* 4.

Proof. The graph's partition dimension of Minocyline drug structure less than equal to 4. To demonstrate this point, we picked a set of cardinality 4 and stated as $R(G) = \{R_1, R_2, R_3, R_4\}$, where $R_1 = \{v_{20}\}$, $R_2 = \{v_{28}\}$, $R_3 = \{v_{33}\}$ and $R_4 = V(G)\backslash\{v_{20}, v_{28}, v_{33}\}$. To demonstrate this statement true, we have included representations of each node of the Minocyline drug structure except v_{20}, v_{28} and v_{33} in Table 5.

Table 5. Representations of the vertices with respect to R.

$r(v_i\|R)$	R_1	R_2	R_3	R_4	Range of i
v_i	$i+1$	$11-i$	$i+2$	0	$i = 1, 2$
v_i	$i+1$	$11-i$	$i+1$	0	$i = 3, ..., 7$
v_i	$i+1$	$13-i$	$i+1$	0	$i = 8, 9$
v_i	$i+1$	$13-i$	$19-i$	0	$i = 10$
v_i	$21-i$	$i-9$	$19-i$	0	$i = 11, ..., 17$
v_i	$i-15$	$i-9$	$i-27$	0	$i = 18, 19$
v_i	$i-20$	$i-10$	$i-16$	0	$i = 21, 22$
v_i	$i-19$	$33-i$	$29-i$	0	$i = 23, 24$
v_i	$31-i$	$33-i$	$31-i$	0	$i = 25$
v_i	$34-i$	$31-i$	$34-i$	0	$i = 26$
v_i	$37-1$	$33-i$	$37-i$	0	$i = 27$
v_i	$i-18$	$i-28$	$i-20$	0	$i = 29, 30$
v_i	$40-i$	$37-i$	$37-i$	0	$i = 31$
v_i	$38-1$	$40-i$	$36-i$	0	$i = 32$
v_i	$39-i$	$43-i$	$35-i$	0	$i = 34$
v_i	$41-i$	$45-i$	$37-i$	0	$i = 35$

Each node of graph of the Minocyline medication structure's given positions is unique and meets the specifications of the partition locating set. This demonstrated that the partition locating number is

correct.

Hence, proved that $pd\left(G_{\text{Minocyline}}\right) \leq 4$.

Raloxifene structure's order and size are $|V\left(G_{\text{Raloxifene}}\right)| = 34$, $|E\left(G_{\text{Raloxifene}}\right)| = 38$, respectively.The node and bond set of the Raloxifene drug structure are shown below. Furthermore, Figure 12 depicts the molecular graph of Raloxifene and labeling employed in our findings.

$$V\left(G_{\text{Raloxifene}}\right) = \{v_i : i = 1, 2, \ldots, 34\},$$
$$E\left(G_{\text{Raloxifene}}\right) = \{v_i v_{i+1} : i = 1, 2, \ldots, 14, 18, \ldots, 31\} \cup \{v_1 v_6,\ v_{10} v_{15},$$
$$v_{13} v_{16},\ v_{16} v_{17},\ v_{16} v_{18},\ v_{18} v_{26},\ v_{19} v_{24},\ v_{22} v_{34},\ v_{27} v_{32},\ v_{18} v_{26},\ v_{30} v_{33}\}.$$

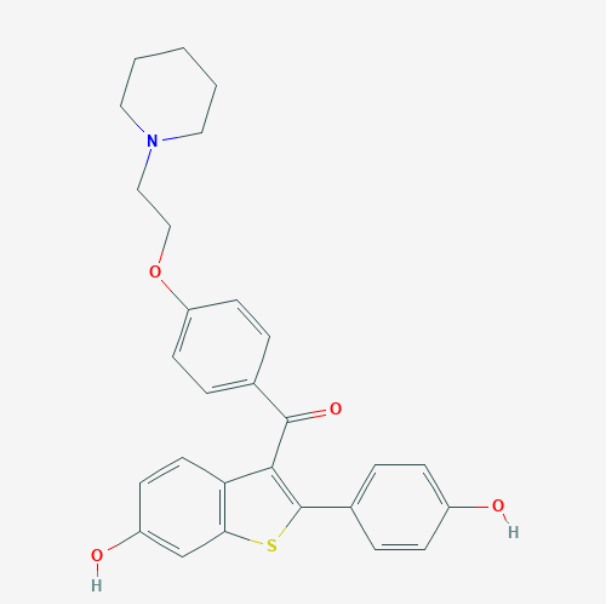

Figure 11. Chemical structure of Raloxifene drug.

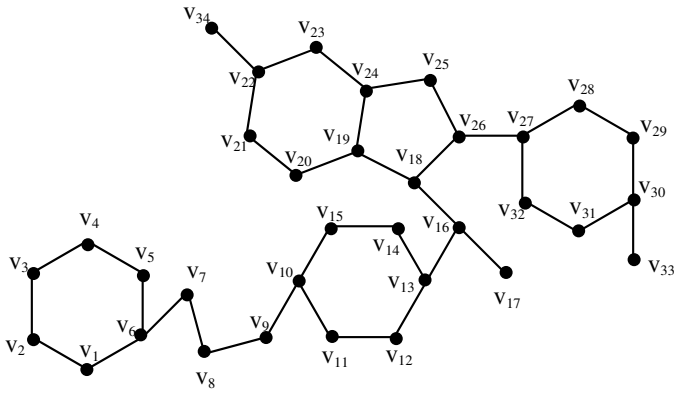

Figure 12. Graph of Raloxifene drug structure shown in the Figure 11.

Theorem 2.6. *Let G be a graph of Raloxifene drug structure. Then the partition locating number of G is less than equal to* 4.

Proof. The graph's partition dimension of Raloxifene drug structure is 4. To demonstrate this point, we picked a set of cardinality 4 and stated as $R(G) = \{R_1, R_2, R_3, R_4\}$, where $R_1 = \{v_{20}\}$, $R_2 = \{v_{28}\}$, $R_3 = \{v_{33}\}$ and $R_4 = V(G)\backslash\{v_{20}, v_{28}, v_{33}\}$ .To demonstrate this statement true, we have included representations of each node of the Raloxifene drug structure except v_{20}, v_{28} and v_{33} in Table 6.

Table 6. Representations of the vertices w.r.t. R.

$r(v_i\|R)$	R_1	R_2	R_3	R_4	Range of i
v_i	$i-1$	$i+5$	$14-i$	0	$i = 1, 2$
v_i	$i-1$	$11-i$	$18-i$	0	$i = 3, 4$
v_i	$i-4$	$11-i$	$18-i$	0	$i = 5$
v_i	$i-5$	$11-i$	$18-i$	0	$i = 6, ..., 10$
v_i	$i-5$	$i-11$	$18-i$	0	$i = 12, 13$
v_i	$21-i$	$17-i$	$i-8$	0	$i = 14, 15$
v_i	$i-7$	$i-13$	$i-12$	0	$i = 16, 17$
v_i	$i-8$	$i-14$	$i-15$	0	$i = 18, 19, 21, 22$
v_i	$36-i$	$30-i$	$28-i$	0	$i = 23, 24$
v_i	$i-15$	$i-21$	$\|28-i\|$	0	$i = 26, 27, 29, 30$
v_i	$45-i$	$39-i$	$34-i$	0	$i = 31, 32$
v_i	$49-i$	$43-i$	$i-30$	0	$i = 34$

Each node of graph of the Raloxifene medication structure's given positions is unique and meets the specifications of the partition locating set. This demonstrated that the metric locating number is correct.

Hence, proved that $pd(G_{\text{Raloxifene}}) \leq 4$.

3. Conclusions

Breast cancer is one of the primary causes of cancer worldwide and the second biggest cause of cancer-related deaths in women (BC). Metastasis development is primarily linked to mortality. Therefore, it is crucial for public health that the mechanisms involved in metastasis formation are identified. Pollution and the chemical environment are among the risk factors that are being indicated as impacting the signaling pathways involved in the formation and growth of metastatic tumor cells. In this research, we consider various cancer drugs structures, computed the partition dimension, and proved that the partition dimension of Podophylb toxin and Pterocellin is 3 and the upper bound of the partition dimension of Daunorubicin, Deguolin, Minocycline, and Raloxifene is 4 as shown in our main findings section. This can help to understand the chemical structure of these various cancer drugs or formulas more deeply.

Acknowledgments

This work was supported by the National Science Foundation of China (11961021 and 11561019), Guangxi Natural Science Foundation (2020GXNSFAA159084), and Hechi University Research Fund for Advanced Talents (2019GCC005).

Conflict of interest

All authors declare no relationships, financial, or commercial conflicts of interest in this paper.

References

1. B. Figuerola, C. Avila, The phylum bryozoa as a promising source of anticancer drugs, *Mar. Drugs*, **17** (2019), 477. https://doi.org/10.3390/md17080477
2. L. J. Kristjanson, T. Ashcroft, The family's cancer journey, *Cancer Nurs.*, **17** (1994), 1–17. https://doi.org/10.1097/00002820-199402000-00001
3. S. Kumar, M. K. Ahmad, M. Waseem, A. K. Pandey, Drug targets for cancer treatment: an overview, *Med. Chem.*, **5** (2015), 115123. https://doi.org/10.4172/2161-0444.1000252
4. R. C. Richie, J. O. Swanson, Breast cancer: a review of the literature, *J. Insur. Med.*, **35** (2003), 85–101. Available from: https://www.aaimedicine.org/journal-of-insurance-medicine/jim/2003/035-02-0085.pdf.
5. A. G. Waks, E. P. Winer, Breast cancer treatment, *JAMA*, **321** (2019), 288–300. https://doi.org/10.1001/jama.2018.19323
6. S. Khuller, B. Raghavachari, A. Rosenfeld, Landmarks in graphs, *Discrete Appl. Math.*, **70** (1996), 217–229. https://doi.org/10.1016/0166-218X(95)00106-2
7. M. F. Nadeem, M. Hassan, M. Azeem, S. U. Khan, M. R. Shaik, M. A. F. Sharaf, et al., Application of resolvability technique to investigate the different polyphenyl structures for polymer industry, *J. Chem.*, **2021** (2021). https://doi.org/10.1155/2021/6633227
8. A. Ali, W. Nazeer, M. Munir, S. M. Kang, M-polynomials and topological indices of zigzagand rhombic benzenoid systems, *Open Chem.*, **16** (2018), 73–78. https://doi.org/10.1515/chem-2018-0010
9. S. Hayat, S. Wang, J. B. Liu, Valency-based topological descriptors of chemical networks and their applications, *Appl. Math. Modell.*, **60** (2018), 164–178. https://doi.org/10.1016/j.apm.2018.03.016
10. S. Kavitha, J. Abraham, M. Arockiaraj, J. Jency, K. Balasubramanian, Topological characterization and graph entropies of tessellations of kekulene structures: existence of isentropic structures and applications to thermochemistry, nuclear magnetic resonance, and electron spin resonance, *J. Phys. Chem. A*, **125** (2021), 8140–8158. https://doi.org/10.1021/acs.jpca.1c06264
11. M. K. Jamil, M. Imran, K. A. Sattar, Novel face index for benzenoid hydrocarbons, *Mathematics*, **8** (2020), 312. https://doi.org/10.3390/math8030312

12. M. F. Nadeem, M. Azeem, H. M. A. Siddiqui, Comparative study of zagreb indices for capped, semi-capped, and uncapped carbon nanotubes, *Polycyclic Aromat. Compd.*, **42** (2022), 3545–3562. https://doi.org/10.1080/10406638.2021.1890625

13. M. F. Nadeem, M. Imran, H. M. A. Siddiqui, M. Azeem, A. Khalil, Y. Ali, Topological aspects of metal-organic structure with the help of underlying networks, *Arabian J. Chem.*, **14** (2021), 103157. https://doi.org/10.1016/j.arabjc.2021.103157

14. A. Ahmad, A. N. A. Koam, M. H. F. Siddiqui, M. Azeem, Resolvability of the starphene structure and applications in electronics, *Ain Shams Eng. J.*, **13** (2022), 101587. https://doi.org/10.1016/j.asej.2021.09.014

15. A. Sebö, E. Tannier, On metric generators of graphs, *Math. Oper. Res.*, **29** (2004), 191–406. https://doi.org/10.1287/moor.1030.0070

16. P. J. Slater, Leaves of trees, *Congr. Numer*, **14** (1975), 549–559.

17. P. Singh, S. Sharma, S. K. Sharma, V. K. Bhat, Metric dimension and edge metric dimension of windmill graphs, *AIMS Math.*, **6** (2021), 9138–9153. https://doi.org/10.3934/math.2021531

18. A. E. Moreno, I. G. Yero, J. A. R. Velazquez, On the (k,t)-metric dimension of graphs, *Comput. J.*, **64** (2021), 707–720. https://doi.org/10.1093/comjnl/bxaa009

19. S. Pirzada, M. Aijaz, On graphs with same metric and upper dimension, *Discrete Math. Algorithms Appl.*, **13** (2021), 2150015. https://doi.org/10.1142/S1793830921500154

20. M. Azeem, M. F. Nadeem, Metric-based resolvability of polycyclic aromatic hydrocarbons, *Eur. Phys. J. Plus*, **136** (2021), 395. https://doi.org/10.1140/epjp/s13360-021-01399-8

21. S. Imran, M. K. Siddiqui, M. Imran, M. Hussain, On metric dimensions of symmetric graphs obtained by rooted product, *Mathematics*, **6** (2018), 191. https://doi.org/10.3390/math6100191

22. A. N. Koam, A. Ahmad, M. E. Abdelhag, M. Azeem, Metric and fault-tolerant metric dimension of hollow coronoid, *IEEE Access*, **9** (2021), 81527–81534. https://doi.org/10.1109/ACCESS.2021.3085584

23. A. N. Koam, A. Ahmad, M. S. Alatawi, M. F. Nadeem, M. Azeem, Computation of metric-based resolvability of quartz without pendant nodes, *IEEE Access*, **9** (2021), 151834–151840. https://doi.org/10.1109/ACCESS.2021.3126455

24. K. Anitha, R. A. Devi, M. Munir, K. S. Nisar, Metric dimension of rough graphs, *Int. J. Nonlinear Anal. Appl.*, **12** (2021), 1793–1806. https://doi.org/10.22075/ijnaa.2021.5891

25. M. Moscarini, Computing a metric basis of a bipartite distance-hereditary graph, *Theor. Comput. Sci.*, **900** (2022), 20–24. https://doi.org/10.1016/j.tcs.2021.11.015

26. A. N. A. Koam, A. Haider, M. A. Ansari, Pseudo-metric on KU-algebras, *Korean J. Math.*, **27** (2019), 131–140. https://doi.org/10.11568/kjm.2019.27.1.131

27. A. Ahmad, M. Baca, S. Sultan, On the minimal doubly resolving sets of Harary graph, *Acta Math. Universitatis Comenianae*, **89** (2019), 123–129. Available from: http://www.iam.fmph.uniba.sk/amuc/ojs/index.php/amuc/article/view/1032.

28. A. Ahmad, M. Baca, S. Sultan, Computing the metric dimension of Kayak Paddles graph and Cycles with chord, *Proyecciones (Antofagasta, On line)*, **39** (2020), 287–300. https://doi.org/10.22199/issn.0717-6279-2020-02-0018

29. A. Ahmad, M. Baca, S. Sultan, Minimal doubly resolving sets of Necklace graph, *Math. Rep.*, **20** (2018), 123–129. Available from: http://www.imar.ro/journals/Mathematical_Reports/Pdfs/2018/2/2.pdf.
30. T. Vetrik, A. Ahmad, Computing the metric dimension of the categorial product of graphs, *Int. J. Comput. Math.*, **94** (2017), 363–371. https://doi.org/10.1080/00207160.2015.1109081
31. A. Ahmad, S. Sultan, On minimal doubly resolving sets of circulant graphs, *Acta Mech. Sin.*, **21** (2017), 6–11. https://doi.org/10.21496/ams.2017.002
32. H. Raza, S. Hayat, X. F. Pan, On the fault-tolerant metric dimension of certain interconnection networks, *J. Appl. Math. Comput.*, **60** (2019), 517–535. https://doi.org/10.1007/s12190-018-01225-y
33. H. Raza, S. Hayat, M. Imran, X. F. Pan, Fault-tolerant resolvability and extremal structures of graphs, *Mathematics*, **7** (2019), 78–97. https://doi.org/10.3390/math7010078
34. H. Raza, S. Hayat, X. F. Pan, On the fault-tolerant metric dimension of convex polytopes, *Appl. Math. Comput.*, **339** (2018), 172–185. https://doi.org/10.1016/j.amc.2018.07.010
35. T. Mahapatra, G. Ghorai, M. Pal, Fuzzy fractional coloring of fuzzy graph with its application, *J. Ambient Intell. Hum. Comput.*, **11** (2020), 5771–5784. https://doi.org/10.1007/s12652-020-01953-9
36. F. Harary, F. H. Melter, On the metric dimension of a graph, *Ars Combin*, **2** (1976), 191–195.
37. J. P. Sturmberg, G. M. McDonnell, How modelling could contribute to reforming primary care—tweaking the ecology of medical care in Australia, *AIMS Med. Sci.*, **3** (2016), 298–311. https://doi.org/10.3934/medsci.2016.3.298
38. R. Zheng, H. Jia, L. Abualigah, Q. Liu, S. Wang, An improved arithmetic optimization algorithm with forced switching mechanism for global optimization problems, *Math. Biosci. Eng.*, **19** (2022), 473–512. https://doi.org/10.3934/mbe.2022023
39. J. B. Liu, M. F. Nadeem, M. Azeem, Bounds on the partition dimension of convex polytopes, *Comb. Chem. High Throughput Screening*, **25** (2020), 547–557. https://doi.org/10.2174/1386207323666201204144422
40. M. Azeem, M. Imran, M. F. Nadeem, Sharp bounds on partition dimension of hexagonal mobious ladder, *J. King Saud Univ. Sci.*, **34** (2022), 101779. https://doi.org/10.1016/j.jksus.2021.101779
41. A. Shabbir, M. Azeem, On the partition dimension of tri-hexagonal alpha-boron nanotube, *IEEE Access*, **9** (2021), 55644–55653. https://doi.org/10.1109/ACCESS.2021.3071716
42. H. M. A. Siddiqui, M. Imran, Computing the metric and partition dimension of h-naphtalenic and VC_5C_7 nanotubes, *J. Optoelectron. Adv. Mater.*, **17** (2015), 790–794.
43. H. M. A. Siddiqui, M. Imran, Computing metric and partition dimension of 2-dimensional lattices of certain nanotubes, *J. Comput. Theor. Nanosci.*, **11** (2014), 2419–2423. https://doi.org/10.1166/jctn.2014.3656